

Shape analysis and computational fluid simulations to assess feline left atrial function and thrombogenesis

Andy L. Olivares¹, Maria Isabel Pons¹, Jordi Mill¹, Jose Novo Matos², Patricia Garcia³, Inma Cerrada², Anna Guy⁴, J. Ciaran Hutchinson⁵, Ian C. Simcock^{4,6}, Owen J. Arthurs^{4,6}, Andrew C. Cook⁷, Virginia Luis Fuentes², and Oscar Camara¹

¹ PhySense, Department of Information and Communication Technologies, Universitat Pompeu Fabra, Barcelona, Spain

² Cardiology Service Head. Royal Veterinary College. UK

³ Institut d'Investigacions Biomèdiques August Pi i Sunyer, Barcelona, Spain

⁴ Department of Radiology, Great Ormond Street Hospital for Children, NHS Foundation Trust, London, UK.

⁵ National Institute for Health Research Great Ormond Street Hospital Biomedical Research Centre, London, UK

⁶ Department of Histopathology, Great Ormond Street Hospital for Children, NHS Foundation Trust, London, UK.

⁷ Institute of Cardiovascular Science, University College London, London, UK.
`oscar.camara@upf.edu`

Abstract. In humans, there is a well-established relationship between atrial fibrillation (AF), blood flow abnormalities and thrombus formation, even if there is no clear consensus on the role of left atrial appendage (LAA) morphologies. Cats can also suffer heart diseases, often leading to an enlargement of the left atrium that promotes stagnant blood flow, activating the clotting process and promoting feline aortic thromboembolism. The majority of pathological feline hearts have echocardiographic evidence of abnormal left ventricular filling, usually assessed with 2D and Doppler echocardiography and standard imaging tools. Actually, veterinary professionals have limited access to advanced computational techniques that would enable a better understanding of feline heart pathologies with improved morphological and haemodynamic descriptors. In this paper, we applied state-of-the-art image processing and computational fluid simulations based on micro-computed tomography images acquired in 24 cases, including normal cats and cats with varying severity of cardiomyopathy. The main goal of the study was to identify differences in the LA/LAA morphologies and blood flow patterns between the analysed cohorts with respect to thrombus formation and cardiac pathology. The obtained results show significant differences between normal and pathological feline hearts, as well as in thrombus vs non-thrombus cases and asymptomatic vs symptomatic cases, while it was not possible to discern between congestive heart failure with thrombus and non-thrombus cases. Additionally, in-silico fluid simulations demonstrated lower LAA blood flow velocities and higher thrombotic risk in the thrombus cases.

Keywords: Feline hearts · thrombus formation · congestive heart failure
· left atrial appendage · computational fluid dynamics

1 Introduction

Cardiac diseases affect most species in the animal kingdom. Atrial fibrillation (AF) is the most frequent arrhythmia in humans, which can lead to irregular contraction of the left atria (LA) and subsequent blood stagnation that can trigger the formation of thrombi, usually in the left atrial appendage (LAA). In other species such as cats, AF rarely occurs due to the small size of their hearts. However, other cardiac diseases such as hypertrophic cardiomyopathy (HCM) is common in felines, with a prevalence of approximately 10–15% [1]. The natural consequence of HCM over time is the enlargement of the left atria, followed by blood flow abnormalities [2] that can potentially lead to blood stasis and thrombus formation. Therefore, LA size has a prognostic importance in cats with cardiomyopathy, being identified as an important risk factor for feline arterial thromboembolism (FATE), which affects around 48% [3] of felines with HCM. Veterinary professionals often use echocardiographic images to assess cardiac function by measuring basic morphological descriptors with 2D standard imaging tools. For instance, it has been established that the maximum diameter of the LA (LAD) is around 16 mm for normal heart cats, while constituting severe risk for LAD larger than 25 mm [4]. Left atrial volumes (LAV) have also been reported in some studies [5, 2], showing differences between healthy and congestive heart failure (CHF) cats (average minimum/maximum LAV in mL): 0.53/1.77 for healthy hearts; and 2.72/3.87 for congestive heart failure cats.

However, to better understand the complex relationship of feline heart morphology and haemodynamics with thrombus formation, more sophisticated descriptors are required. There are several studies in humans using advanced computational techniques to better describe LA and LAA morphologies in relation with the risk of thrombus formation, either with qualitative categories (e.g. chicken-wing et al.) or with more quantitative metrics characterising the ostium (i.e. interface between the LA and the LAA) and LAA shape (e.g., centreline [6]). Additionally, computational fluid simulations are emerging as a powerful tool to investigate the 4D nature of blood flow patterns in the LA, furnishing in-silico indices of thrombogenic risk [7, 8]. Unfortunately, these state-of-the-art techniques have never been applied for the assessment of feline cardiac function. The main goal of this study was to derive advanced 3D shape and haemodynamic descriptors of the feline LA from the analysis and computational modelling of micro-computed tomography (micro-CT) data, available in 24 cats, to identify differences between normal (8 cats) and pathological (16 cats, including congestive heart failure or asymptomatic HCM, and with/without thrombus) cases. The pipeline of the developed methodology is illustrated in Figure 1.

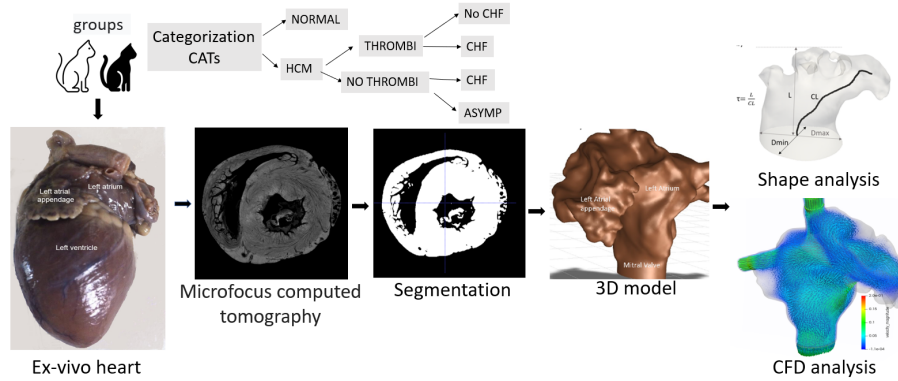


Fig. 1. Computational pipeline to derive morphological and haemodynamic descriptors of the feline hearts. Ex-vivo isolated feline hearts were evaluated with micro-computed tomography (micro-CT) images, from which the left atria were segmented prior to create 3D surface meshes. Then, shape and Computational Fluid Dynamics (CFD) analysis were performed to derive morphological and haemodynamic descriptors. HCM: hypertrophic cardiomyopathy; CHF: congestive heart failure; ASYMP: asymptomatic.

2 Materials and Methods

2.1 Sample description

The present prospective observational post-mortem study was approved by the Clinical Research Ethical Review Board of the Royal Veterinary College (RVC) (URN 2016-1638-3). Ex-vivo isolated feline heart specimens were evaluated by micro-CT at the Great Ormond Street Hospital (GOSH), followed by standard gross and histopathology examinations performed by a board-certified veterinary pathologist at the RVC as the gold standard. Twenty-four hearts were finally processed, including 8 normal (N) hearts and 16 presenting different cardiac diseases: 5 with congestive heart failure (CHF); 5 asymptomatic HCM; and 6 with thrombus⁸).

Micro-computed tomography imaging and staining protocols were performed as previously described for feline hearts [9]. Micro-CT scans were carried out using a Nikon XTH225 ST and a Med-X micro-CT scanner (Nikon Metrology, Tring, UK) based at GOSH.

Reconstructions were carried out using modified Feldkamp filtered back projection algorithms with proprietary software (CTPro3D; Nikon Metrology) and post-processed using VGStudio MAX (Volume Graphics GmbH, Heidelberg, Germany). Whole heart micro-CT scans were reconstructed into an isotropic volume. Isotropic voxel sizes ranged between 19-24 μm , furnishing approximately 900 2D slices per case.

⁸ Note that two cases had both congestive heart failure and thrombus.

2.2 3D surface reconstruction of the left atrium

An in-house script consisting on automatic Otsu’s thresholding techniques, 3D Gaussian smoothing (7 pixels per dimension) and noise reduction with morphological operations implemented in Matlab (R2018b Academic license⁹) was used to segment the whole heart in the micro-CT scans. The LA chamber was then manually extracted from the whole heart segmentation. The resulting LA binary masks (see Figure 1) were introduced into the marching cubes algorithm to build 3D surface meshes. The computational pipeline to create the volumetric meshes required for the fluid simulations was based on Aguado et al. [7]. A Taubin smoothing filter (with scale factors $\lambda = 0.6$, $\mu = -0.53$ and 10 iterations) was applied to the surface meshes using MeshLab¹⁰. Afterwards, the pulmonary veins (PVs) and the mitral valve (MV) were synthetically placed using Mesh-Mixer¹¹ to set up the boundary conditions. Finally, the Gmsh¹² software was used to create the volumetric mesh needed for the fluid solver.

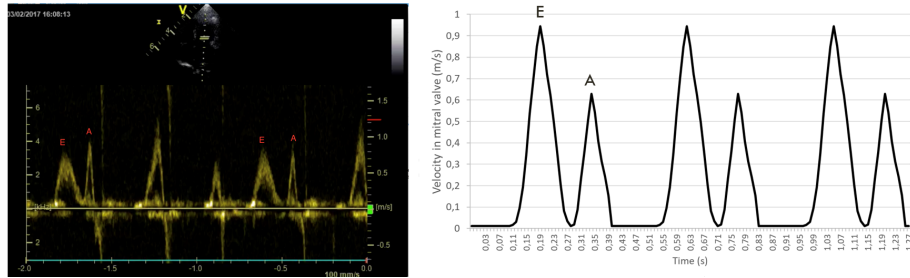


Fig. 2. Doppler echocardiographic record from a cats (left) and transmitral flow velocity applied as the boundary condition in the CFD simulations for this study (right)

2.3 Morphological and haemodynamic descriptors

The surface meshes of all feline hearts were analysed to derive several shape descriptors aiming at characterising the morphology of the LA and LAA, as can be seen in Figure 1. First, volumes of the LA and LAA as well as their ratio (i.e. LAA/LA volume ratio) were estimated. Then, the ostium was manually selected to compute its area (AO) and their maximum/minimum diameters (D_{max} , D_{min} , respectively in Figure 1), which have been related to thrombus formation in humans[10]). Moreover, the LAA centreline (CL in Figure 1) was defined as the line going from the ostium centre to the furthest geodesic point

⁹ <https://mathworks.com/products/matlab.html>

¹⁰ <https://www.meshlab.net>

¹¹ <https://www.meshmixer.com>

¹² <https://www.gmsh.info>

in the LAA, as in [6]. Finally, the centreline length and tortuosity (τ in Figure 1, dividing the length by the height of the LAA, L) were estimated. Several morphological descriptors were normalised by the LA and LAA volumes, as well as for the cat heart weight, to compensate for different size hearts.

Due to computational reasons, in-silico haemodynamics descriptors were only evaluated a subset of the studied dataset, with a total of 10 computational fluid dynamics (CFD) simulations, two for each one of the following categories: normal, asymptomatic HCM with/without thrombus and CHF with/without thrombus. The CFD analysis was performed using the finite volume element method (FVM) in the Ansys Fluent 2019 solver (Ansys Inc, USA)¹³. Blood was modelled as an incompressible Newtonian fluid (density of $\rho= 1060 \text{ kg/m}^3$; dynamic viscosity of $\mu = 0.0035 \text{ Pa}\cdot\text{s}$), using the Navier-Stokes and continuity equations. A generic boundary condition for a cat with 140 bpm was simulated over three cardiac cycles. An velocity wave was applied in the mitral valve (MV) Figure2 and in the pulmonary veins (PVs) the pressure wave was imposed [2]. In addition, the motion of the mitral annular plane excursion in cats with HCM estimated in Spalla et al. [3] was imposed with a dynamic mesh approach. The dynamic mesh method was the spring-based method available in Fluent based on a MV ring function described in the work by Mill et al.[8]. Several haemodynamics descriptors were obtained from CFD simulations, including velocity curves in the LAA ostium and in-silico indices to estimate the risk of thrombus formation. In particular, we computed the endothelial activation potential (ECAP) as the ratio between the oscillatory shear index (OSI) and the time average wall shear (TAWSS), since it highlights regions with low velocities and high complexity of blood flow, thus prone to thrombus generation [7].

Morphological descriptors were analysed with statistical student t-test, Mann-Whitney - Wilcoxon and χ^2 tests when appropriate, with a level of significance of 0.05. The main objective of the statistical study was to identify shape differences between the following cohorts (number of cases): normal (8) vs cardiomyopathy (16); thrombus (6) vs non-thrombus (10); asymptomatic HCM (5) vs symptomatic (CHF-Thrombus) (11); and CHF with thrombus (2) vs CHF non-thrombus (5).

3 Results and discussion

Table 1 shows the clinical and morphological descriptors comparing normal and cardiomyopathy feline hearts. There were statistically significant differences between normal and pathological cases in the majority of volumetric indices (both in the LA and the LAA) and in the ostium area, with larger values for cardiomyopathy cases, as expected. The LAA centrelines were larger and less tortuous for pathological cats, reaching statistical difference for the length of the centreline.

Significant differences between thrombus and non-thrombus cases were found for the LAA and LA volumes, ostium area, centreline length and tortuosity, as

¹³ <http://www.ansys.com>

Table 1. Descriptors of normal (n = 8) vs cardiomyopathy (n = 16) cats. HW: Heart weight (g); LAV/LAAv (mL): Left Atrial and Appendage volumes; AO (mm^2): Area of Ostium; CL (mm), τ : LAA centreline length and tortuosity, respectively; Age (years). Results are presented as mean \pm standard deviation. * Data was not available for all cases.

Descriptors	Normal	Cardiomyopathy	p-value
HW	15.15 \pm 2.67	22.41 \pm 6.62	0.001
LAAv	0.23 \pm 0.11	1.07 \pm 0.85	p<0.001
LAv	1.13 \pm 0.50	3.78 \pm 1.99	p<0.001
LAAv/LAv(%)	21.78 \pm 8.58	27.59 \pm 14.79	0.70
AO	37.60 \pm 14.48	117.60 \pm 55.08	p<0.001
AO/LAv	34.54 \pm 14.38	33.75 \pm 10.11	0.89
AO/LAAv	165.24 \pm 55.43	134.54 \pm 45.52	0.20
AO/Heart weight	2.57 \pm 1.16	5.60 \pm 3.03	0.002
CL (mm)	8.09 \pm 1.77	14.46 \pm 5.60	0.01
τ	0.84 \pm 0.07	0.73 \pm 0.24	0.31
Gender*	Female (3) (37.50%) Male (5) (62.50%)	Female (5) (33.33%) Male (10) (66.67%)	1.00
Neutered*	Yes (2) (33.33%) No (4) (66.67%)	Yes (12) (80%) No (3) (20%)	0.13
Age*	6.34 \pm 4.83	7.93 \pm 3.75	0.46

Table 2. Descriptors of thrombus (n = 6) vs non-thrombus (n = 10) cats. HW: Heart weight (g); LAV/LAAv (mL): Left Atrial and Appendage volumes; AO (mm^2): Area of Ostium; CL (mm), τ : LAA centreline length and tortuosity, respectively; Age (years). Results are presented as mean \pm standard deviation. * Data was not available for all cases.

Descriptors	Thrombus	Non-thrombus	p-value
HW	24.07 \pm 8.50	21.42 \pm 5.48	0.52
LAAv	1.76 \pm 1.07	0.67 \pm 0.30	0.02
LAv	5.23 \pm 2.08	2.92 \pm 1.39	0.04
LAAv/LAv(%)	35.02 \pm 23.15	23.14 \pm 2.79	0.49
AO	157.92 \pm 65.66	93.41 \pm 30.45	0.04
AO/LAv	31.56 \pm 11.75	35.06 \pm 9.42	0.55
AO/LAAv	105.50 \pm 38.32	151.97 \pm 41.69	0.04
AO/Heart weight	7.06 \pm 3.31	4.72 \pm 2.62	0.18
CL (mm)	19.42 \pm 4.31	11.49 \pm 3.97	0.004
τ	0.60 \pm 0.26	0.81 \pm 0.20	0.02
Gender*	Female (3) (50%) Male (3) (50%)	Female (2) (22.22%) Male (7) (77.78%)	0.58
Neutered*	Yes (4) (66.67%) No (2) (33.33%)	Yes (8) (88.89%) No (1) (11.11%)	0.53
Age*	8.33 \pm 3.08	7.67 \pm 4.30	0.73

well as for the ostium area normalised by the LAA volume (see Table 2). In general, we observed larger LA and LAA volumes, as well as ostium areas in

Table 3. Descriptors of asymptomatic (n = 5) vs symptomatic (CHF-Thrombus) (n = 11) cats. HW: Heart weight (g); LAv/LAAv (mL): Left Atrial and Appendage volumes; AO (mm^2): Area of Ostium; CL (mm), τ : LAA centreline length and tortuosity, respectively; Age (years). Results are presented as mean \pm standard deviation. * Data was not available for all cases.

Descriptors	Asymptomatic	Symptomatic	p-value
HW	20.16 \pm 6.47	23.44 \pm 6.73	0.38
LAAv	0.57 \pm 0.31	1.31 \pm 0.93	0.05
LAv	2.31 \pm 1.34	4.45 \pm 1.90	0.03
LAAv/LAv(%)	24.61 \pm 3.16	28.95 \pm 17.82	0.66
AO	92.66 \pm 40.67	128.94 \pm 58.62	0.15
AO/LAv	42.34 \pm 6.76	29.84 \pm 9.02	0.01
AO/LAAv	175.38 \pm 44.94	115.98 \pm 32.98	0.04
AO/Heart weight	5.19 \pm 3.71	5.78 \pm 2.85	0.51
CL (mm)	9.41 \pm 2.03	16.76 \pm 5.18	0.001
τ	0.89 \pm 0.06	0.65 \pm 0.26	0.01
Gender*	Female (1) (25%) Male (3) (75%)	Female (4) (36.36%) Male (7) (63.64%)	1.00
Neutered*	Yes (3) (75%) No (1) (25%)	Yes (9) (81.82 %) No (2) (18.18%)	1.00
Age*	8.75 \pm 6.60	7.64 \pm 2.50	0.76

thrombus vs non-thrombus cases, in agreement with values reported in human studies [10]. The possible hypothesis is that large ostia imply lower velocities in the LAA and then potential blood stasis. However, the ostium areas, when normalised by the LA and LAA volumes, were higher for non-thrombus cases, which has also been reported [11]. In this scenario, we are roughly considering the amount of flow getting into the LAA, accounting for the LA volume. A potential alternative hypothesis for thrombus generation would be that smaller ostia, compared to LA and LAA volumes, would prevent a proper washing of the blood flow out of the LAA, also promoting stasis. Finally, larger LAA centreline length and smaller tortuosity values were also found from cats with thrombus, in agreement with this second hypothesis.

Table 3 summarises clinical and morphological descriptors comparing asymptomatic HCM (A-HCM) and symptomatic HCM cases. The LA volume values in our study were comparable with those reported by Duler et al. [5]. LA and LAA volumes and ostium areas were larger for symptomatic cases, also having larger and less tortuous LAA centrelines. As mentioned above, when normalising the ostium area with the LA and LAA volumes (the former at the level of statistical significance, $p = 0.05$), symptomatic cases presented smaller values, following the washing hypothesis for blood stasis. We did not observe significant differences when comparing the clinical and morphological descriptors of CHF cases with and without thrombus, likely due to the small number of samples (two and five, respectively).

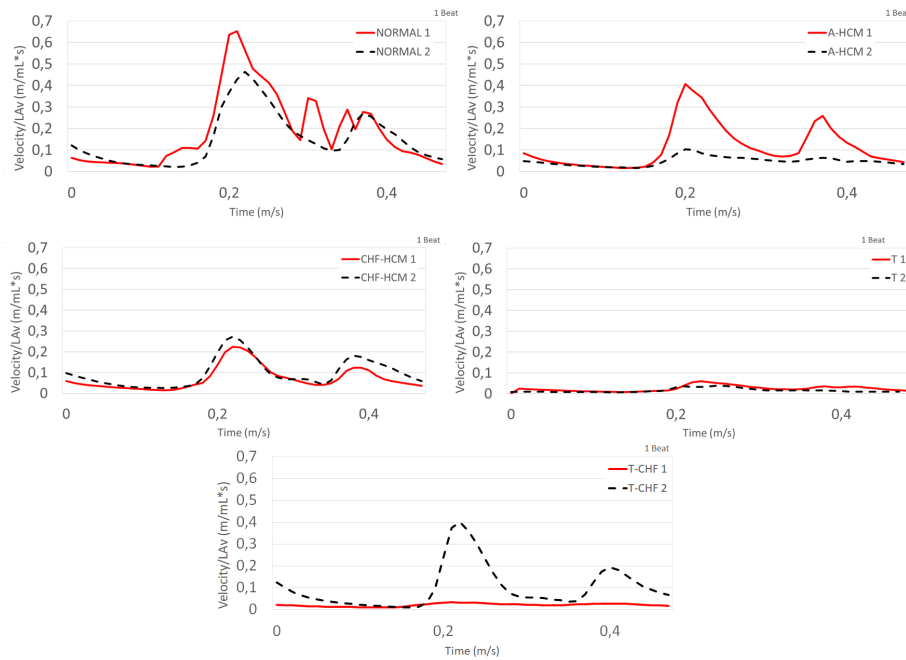


Fig. 3. Blood velocity profiles at the left atrial appendage (LAA) ostium (normalised by the LA volume) from computational fluid simulations for two cases representing each feline heart category. CHF: congestive heart failure; A-HCM: asymptomatic hypertrophic cardiomyopathy; T: thrombus.

Figure 3 shows the fluid simulation results in the ten studied cases. It can be observed how the blood flow velocity profiles at the LAA ostium, normalised by the LA volume, showed the expected behaviour: higher and lower values for normal and thrombus cases, respectively, with the non-thrombus CHF somewhere in the middle. On the other hand, the asymptomatic HCM cases different velocity magnitudes in the two analysed cases, being difficult to draw any conclusion.

The ECAP distribution is also illustrated in Figure 4, showing larger areas with higher values of ECAP (i.e., complex flows and low velocities; red-green areas) in cats with thrombus.

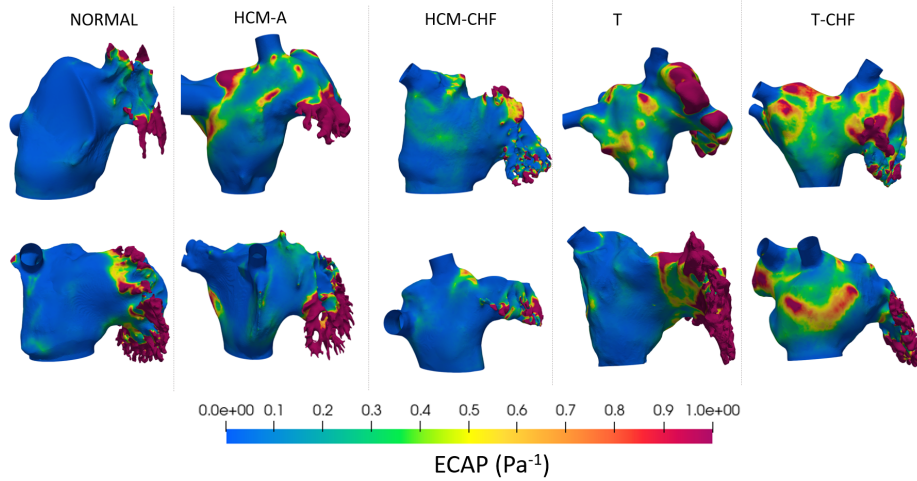


Fig. 4. Endothelial Cell Activation Potential (ECAP) maps from the in-silico fluid simulations, for one case representing each feline heart category. Red-green areas represent areas with high ECAP values, (lower blood flow velocities and more complex flow), thus more prone to thrombus formation. CHF: congestive heart failure; A-HCM: asymptomatic hypertrophic cardiomyopathy; T: thrombus.

4 Conclusions

The present research study is the first attempt to applying advanced computational tools on high-resolution images of in normal and cardiomyopathy feline hearts to better understand the complex relation between left atrial morphology, blood flow patterns and thrombus formation. Morphological differences were found in several descriptors between normal and pathological hearts, as well as in thrombus vs non-thrombus cases, even if further investigations are required to reconcile different hypothesis for the role of LAA ostium in blood stasis. Nevertheless, the trends observed in the studied feline hearts (e.g., larger LA volumes in cardiomyopathies vs normals or CHF vs asymptomatic, larger ostium area for thrombus vs non-thrombus) are similar to those found in humans. In-silico indices from fluid simulations confirmed differences in blood flow patterns in these cohorts, with lower velocities in thrombus vs non-thrombus cases. On the other hand, the asymptomatic HCM and CHF hearts were not possible to clearly differentiate from the hemodynamics descriptors. Future work will focus on analysing a larger population of cases, including data from other species such as dogs; these studies could contribute to improve the health of our loved companions as well as to create new knowledge that can potentially be translated to human data.

References

- [1] Arisara Kiatsilapanan et al. “Assessment of left atrial function in feline hypertrophic cardiomyopathy by using two- dimensional speckle tracking echocardiography”. In: *BMC Veterinary Research* 3 (2020), pp. 1–10.
- [2] Karsten E. Schober et al. “Echocardiographic evaluation of left ventricular diastolic function in cats: Hemodynamic determinants and pattern recognition”. In: *Journal of Veterinary Cardiology* 17 (2015), pp. 102–133.
- [3] Ilaria Spalla et al. “Prognostic value of mitral annular systolic plane excursion and tricuspid annular plane systolic excursion in cats with hypertrophic cardiomyopathy”. In: *Journal of Veterinary Cardiology* 20 (2018).
- [4] S M Johns et al. “Left Atrial Function in Cats with Left-Sided Cardiac Disease and Pleural Effusion or Pulmonary Edema”. In: *Journal of Veterinary Internal Medicine* 26 (2012), pp. 1134–1139.
- [5] L. Duler et al. “Left atrial size and volume in cats with primary cardiomyopathy with and without congestive heart failure”. In: *Journal of Veterinary Cardiology* 24 (2019), pp. 36–47.
- [6] Ibai Genua et al. “Centreline-based shape descriptors of the left atrial appendage in relation with thrombus formation”. In: *Statistical Atlases and Computational Models of the Heart. MICCAI, STACOM 2018*. 2018.
- [7] Ainhoa M. Aguado et al. “In silico optimization of left atrial appendage Occluder implantation using interactive and modeling tools”. In: *Frontiers in Physiology* 10 (2019).
- [8] Jordi Mill et al. “Impact of Flow Dynamics on Device-Related Thrombosis After Left Atrial Appendage Occlusion”. In: *Canadian Journal of Cardiology* 36 (2020).
- [9] Ian C. Simcock et al. “Investigation of optimal sample preparation conditions with potassium triiodide and optimal imaging settings for microfocus computed tomography of excised cat hearts”. In: *American Journal of Veterinary Research* 81 (4 2020).
- [10] Yonggu Lee et al. “Comparison of Morphologic Features and Flow Velocity of the Left Atrial Appendage Among Patients With Atrial Fibrillation Alone, Transient Ischemic Attack, and Cardioembolic Stroke”. In: *The American Journal of Cardiology* 119 (2017), pp. 1596–1604.
- [11] Irfan M. Khurram et al. “Relationship between left atrial appendage morphology and stroke in patients with atrial fibrillation”. In: *Heart Rhythm* 10.12 (2013), pp. 1843–1849.